

Formation and Transformation of Clathrate Hydrates under Interstellar Conditions

Jyotirmoy Ghosh, Gaurav Vishwakarma, Rajnish Kumar,* and Thalappil Pradeep*

Cite This: <https://doi.org/10.1021/acs.accounts.3c00317>

Read Online

ACCESS |

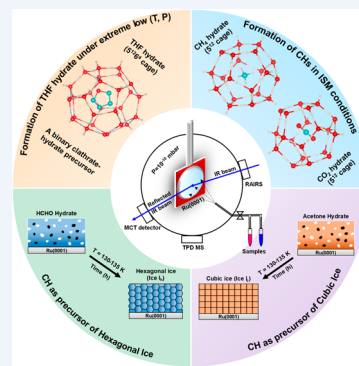
Metrics & More

Article Recommendations

CONSPECTUS: Continuing efforts by many research groups have led to the discovery of ~240 species in the interstellar medium (ISM). Observatory- and laboratory-based astrochemical experiments have led to the discovery of these species, including several complex organic molecules (COMs). Interstellar molecular clouds, consisting of water-rich icy grains, have been recognized as the primordial sources of COMs even at extremely low temperatures (~10 K). Therefore, it is paramount to understand the chemical processes of this region, which may contribute to the chemical evolution and formation of new planetary systems and the origin of life.

This Account discusses our effort to discover clathrate hydrates (CHs) of several molecules and their structural varieties, transformations, and kinetics in a simulated interstellar environment. CHs are nonstoichiometric crystalline host–guest complexes in which water molecules form cages of different sizes to entrap guest molecules. CHs are abundant on earth and require moderate temperatures and high pressures for their formation. Our focus has been to form CHs at extremely low pressure and temperature as in the ISM, although their existence under such conditions has been a long-standing question since water and guest molecules (CH₄, CO₂, CO, etc.) exist in space. In multiple studies conducted at ~10⁻¹⁰ mbar, we showed that CH₄, CO₂, and C₂H₆ hydrates could be formed at 30, 10, and 60 K, respectively. Well-defined IR spectroscopic features supported by quantum chemical simulations and temperature-programmed desorption mass spectrometric analyses confirmed the existence of the S¹² (for CH₄ and CO₂) and S¹²6² (for C₂H₆) CH cages. Mild thermal activation for long periods under ultrahigh vacuum (UHV) allowed efficient molecular diffusion, which is crucial for forming CHs. We also explored the formation of THF hydrate (a promoter/stabilizer for binary CHs), and a spontaneous method was found for its formation under UHV. In a subsequent study, we observed a binary THF-CO₂ hydrate and its thermal processing at 130 K leading to the transportation of CO₂ from the hydrate cages to the matrix of amorphous water. The findings imply that such systems possess a dynamic setting that facilitates the movement of molecules, potentially accounting for the chemical changes observed in the ISM. Furthermore, an intriguing fundamental phenomenon is the consequences of these CHs and their dynamics. We showed that preformed acetone and formaldehyde hydrates dissociate to form cubic (I_c) and hexagonal (I_h) ices at 130–135 K, respectively. These unique processes could be the mechanistic routes for the formation of various ices in astrophysical environments.

Other than adding a new entry, namely, CHs, to the list of species found in ISM, its existence opens new directions to astrochemistry, observational astronomy, and astrobiology. Our work provides a molecular-level understanding of the formation pathways of CHs and their transformation to crystalline ices, which sheds light on the chemical evolution of simple molecules to COMs in ISM. Furthermore, CHs can be potential candidates for studies involving radiation, ionization, and electron impact to initiate chemical transformations between the host and guest species and may be critical in understanding the origin of life.



in Ultrahigh Vacuum under Cryogenic Conditions. *J. Phys. Chem. Lett.* **2020**, *11*, 26–32.² This work reported a unique crystallization process of cubic ice (ice I_c) involving the dissociation of preformed acetone hydrate in UHV.

KEY REFERENCES

- 1. Ghosh, J.; Methikkalam, R. R. J.; Bhui, R. G.; Ragupathy, G.; Choudhary, N.; Kumar, R.; Pradeep, T. Clathrate Hydrates in Interstellar Environment. *Proc. Natl. Acad. Sci. U.S.A.* **2019**, *116*, 1526–1531.¹ This work reported the experimental evidence of CH₄ and CO₂ clathrate hydrates (CHs) at extremely low pressure (10⁻¹⁰ mbar) under cryogenic conditions, relevant to the interstellar medium (ISM).
- 2. Ghosh, J.; Bhui, R. G.; Vishwakarma, G.; Pradeep, T. Formation of Cubic Ice via Clathrate Hydrate, Prepared

Received: June 3, 2023

Received: June 3, 2023

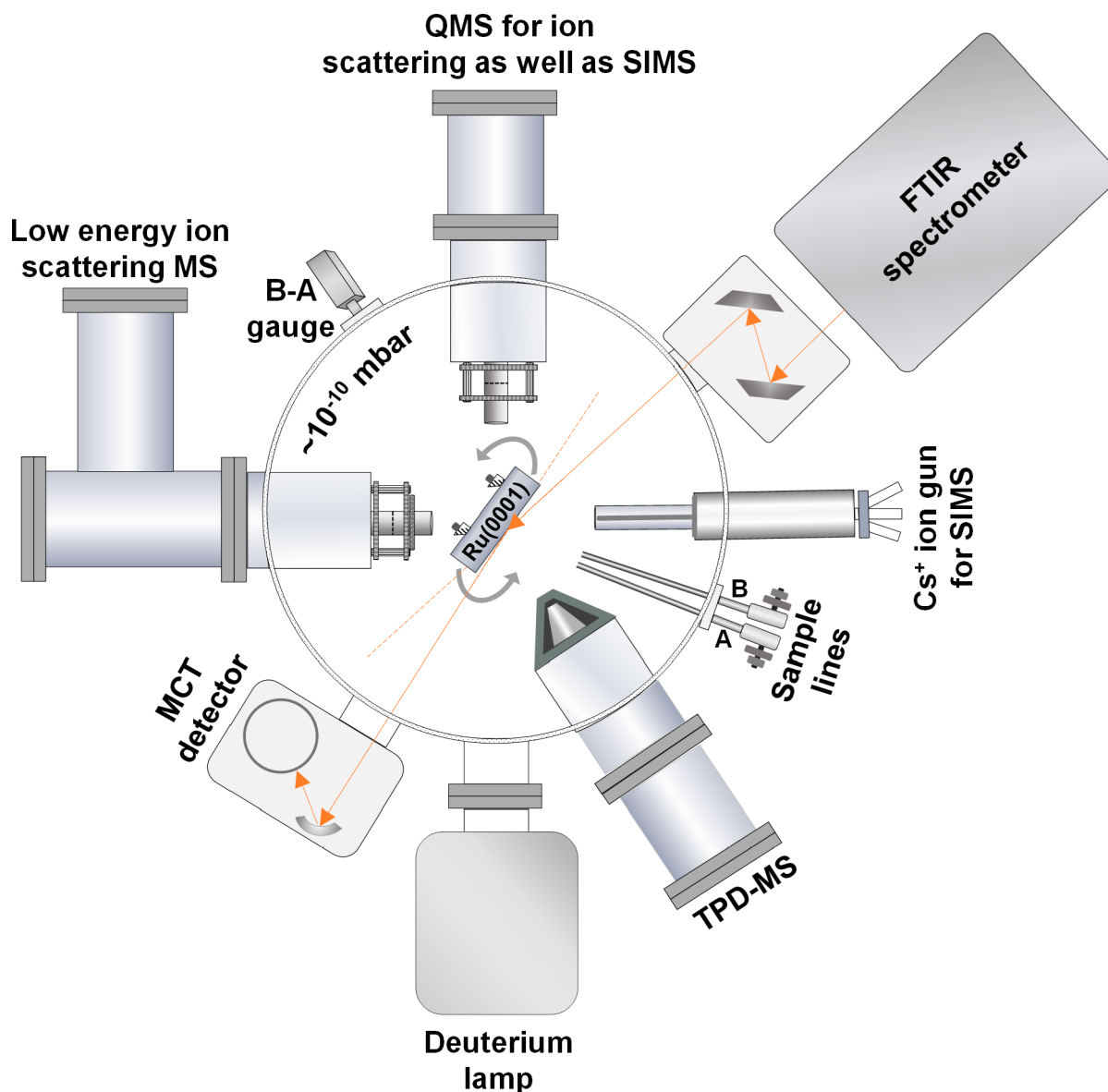


Figure 1. Schematic representation of a custom-built UHV instrument. The current representation depicts the orientation of the substrate suitable for RAIRS measurements. Here, several minor components are not shown for clarity. Adapted with permission from ref 57. Copyright 2023 American Chemical Society.

- Ghosh, J.; Vishwakarma, G.; Das, S.; Pradeep, T. Facile Crystallization of Ice I_h via Formaldehyde Hydrate in Ultrahigh Vacuum under Cryogenic Conditions. *J. Phys. Chem. C* **2021**, *125*, 4532–4539.³ This work showed that a stable hexagonal crystalline ice (ice I_h) can be obtained based on the dissociation of formaldehyde hydrate in UHV.
- Ghosh, J.; Bhui, R. G.; Ragupathy, G.; Pradeep, T. Spontaneous Formation of Tetrahydrofuran Hydrate in Ultrahigh Vacuum. *J. Phys. Chem. C* **2019**, *123*, 16300–16307.⁴ This work demonstrated the formation of tetrahydrofuran (THF) hydrate in UHV, which was a diffusion-controlled process, revealed by the isothermal kinetic measurements.

1. INTRODUCTION

The interstellar medium (ISM) is not empty but contains diffuse clouds, composed of gaseous species, particulate matter, and dust particles.^{5,6} To date, ~ 240 different molecules have

been found in these clouds, making ISM exceedingly diverse and a host to rich chemistry.⁷ Molecular H_2 is the most abundant species found in ISM along with common terrestrial molecular species, molecular ions, radicals, complex organic molecules (COMs), and polycyclic aromatic hydrocarbons (PAHs).⁵ ISM is extremely cold (~ 10 K); therefore, most of these gaseous species get accreted onto the dust surfaces to form icy grain mantles. Ice in the ISM context refers to all condensed molecular solids. Such interstellar icy dust particles are considered to be the birthplace of COMs even at such low temperatures; therefore, it is important to study the associated chemistry.^{5,6} Several studies^{8–10} involving absorption IR spectroscopy were used to characterize the compositions of interstellar ice, and water is found to be the major constituent, followed by CO_2 , CO , CH_3OH , NH_3 , and CH_4 .⁶ This interstellar ice is known to have two different phases, namely, water-rich and water-poor analogs.⁶ The water-rich phase consists of mostly water and CO_2 , alongside small amounts of

NH₃ and CH₄ ices, whereas the water-poor phase contains mostly CO, CO₂, and CH₃OH.⁶ In interstellar environments, the coexistence of all of these molecules along with water in the condensed phase presents a perfect recipe for clathrate hydrates (CHs), a unique molecular species yet to be detected in ISM, and this Account addresses that gap.

CHs are nonstoichiometric crystalline host–guest complexes, where water molecules form a cage-like structure to entrap different guest species to gain stabilization by the host–guest interaction.^{11,12} Their structures are dependent on the nature of guest species, and the most commonly occurring structures are referred to as structure I (sI), structure II (sII), and structure H (sH).^{11,12} CHs are also abundant on earth and generally found in permafrost regions, ocean floors, and outer continental shelves as marine sediments.^{11,13} CHs are known to serve as important materials as a sustainable source of energy^{14,15} and for the storage of natural gases with huge entrapment capability,^{14,16} CO₂ sequestration,^{17,18} and seawater desalination.¹⁹ It is also important to understand the nucleation and decomposition behaviors of CHs for flow assurance in subsea pipelines²⁰ and global climate change,¹⁸ respectively.

In general, high pressure and moderate to low temperature are the stabilizing conditions for the nucleation and growth of CHs.¹¹ However, CHs can also form at low pressures and temperatures as per the *P*–*T* phase diagram, and their existence was predicted in the outer solar system²¹ and on the surfaces of Mars and Titan.^{22,23} In the 1980s, CHs were first formed experimentally under vacuum (1.33×10^{-7} mbar) by the codeposition of an appropriate water:oxirane vapor mixture followed by annealing to 120 K.²⁴ Subsequently, other studies were followed, involving a similar vapor deposition method with small proton-acceptor guest species, which stabilizes the CH structure.^{25–28} Ice nanocrystal arrays were also shown to be converted to CH arrays.^{29,30} Under relatively higher vacuum ($\sim 10^{-6}$ mbar), several other CHs were studied such as those of NO,³¹ N₂,^{32,33} O₂,^{32,33} CO,³³ and Ar.³³

There has been speculation about the existence of CHs in comets and other planetary atmospheres due to prevalent temperature and pressure. However, there was no experimental evidence of the formation of CHs in UHV and cryogenic conditions relevant to the interstellar environment before our studies. In this Account, we discuss our experimental effort toward the formation of CHs in a simulated interstellar environment and the associated chemistry, kinetics, and transformation of such structures. This discussion begins with the description of a custom-built UHV instrument for studying CHs, in which an interstellar condition was mimicked. In the next section, we discuss the formation of CH₄, C₂H₆, and CO₂ hydrates under UHV ($\sim 10^{-10}$ mbar) in the 10–60 K range and their characterization by IR spectroscopy, quantum chemical calculations, and mass spectrometry. Then, we demonstrate that the CHs can be converted to different forms of crystalline ice (cubic and hexagonal ice) upon their dissociation. We have provided spectroscopic and electron diffraction evidence in support of the observation of these different crystalline forms of ice. In a later section, we discuss a spontaneous method of forming THF hydrate in UHV, which can promote the formation of binary CHs (a type of CH where two different guest species are trapped in two separate CH cages). Furthermore, we show that it is indeed possible for a binary THF-CO₂ hydrate to form under UHV, which shows the transportation of CO₂ from

CHs to an amorphous solid water (ASW) matrix upon annealing at certain temperatures, suggesting the dynamic nature of these interstellar ice systems, which is a prerequisite for more complex chemistries to occur at such low temperatures. Finally, a conclusion is drawn about the future directions of this emerging field.

2. INSTRUMENTATION AND METHOD

2.1. Experimental Setup

Herein, the experimental details and description of the custom-built UHV instrument for studying CHs are presented, as shown in Figure 1. More details about the instrument can be found in recent papers.^{34–38} The instrument has a cylindrical UHV chamber fitted with turbomolecular pumps backed by oil-free diaphragm pumps. Ionization gauges of the Bayard–Alpert type were used in the UHV range. The base pressure below $\sim 5 \times 10^{-10}$ mbar was achieved after the bake-out. A closed-cycle helium cryostat cooled the Ru(0001) substrate over which ice layers were grown. An electrically resistive heater (25 Ω) was used to heat the substrate, and three temperature sensors such as silicon diode, a thermocouple, and a Pt resistor were used for temperature measurements.

2.2. RAIRS Instrumentation

Our reflection absorption infrared spectroscopy (RAIRS) setup used an IR beam focused on the substrate at an $80 \pm 7^\circ$ incident angle, and the reflected beam was refocused to a liquid-nitrogen-cooled MCT external detector through gold-coated mirrors. All of the RAIRS instrumental components outside UHV were purged continuously with dry nitrogen gas to avoid the spectral background from water and CO₂. In all of the experiments, 2 cm⁻¹ resolution was used with 512 scans in the mid-infrared region (4000–400 cm⁻¹).

2.3. TPD-MS Instrumentation

The TPD-MS module from Extrel CMS was attached to the experimental chamber, and it consists of an electron impact source, mass analyzer, and detector. The ionized gaseous species were focused on the mass analyzer by using a stack of Einzel lenses. For TPD-MS, the temperature ramping was controlled with a Lakeshore temperature controller. A thermocouple sensor was used during the experiments in combination with a Pt sensor. The outputs of both sensors from the temperature controller were given to the mass controller and were recorded by the Merlin software along with selected mass intensities.

2.4. General Experimental Protocol

The general experimental procedure of forming CHs is either codeposition or the sequential deposition of water and CH-forming gases. A high-precision leak valve was used to control the deposition pressure, where water and other gaseous guests were deposited by using two separate inlet lines. Millipore water (18.2 MΩ) was used by purifying with freeze–pump–thaw cycles to deposit 300 monolayers (MLs) of ice; therefore, the substrate does not affect the formation of CH. The monolayer (ML) coverage was calculated by assuming that 1.33×10^{-6} mbar s = 1 ML.^{39,35}

For the deposition of 300 MLs of 1:1 mixed ice, the chamber was backfilled starting from a base pressure of $\sim 5 \times 10^{-10}$ mbar to a total pressure of $\sim 5 \times 10^{-7}$ mbar (the pressure of the specific gas as well as water was 2.5×10^{-7} mbar, individually) and deposited for 10 min. Moreover, a residual gas analyzer was used during the deposition of these molecules,

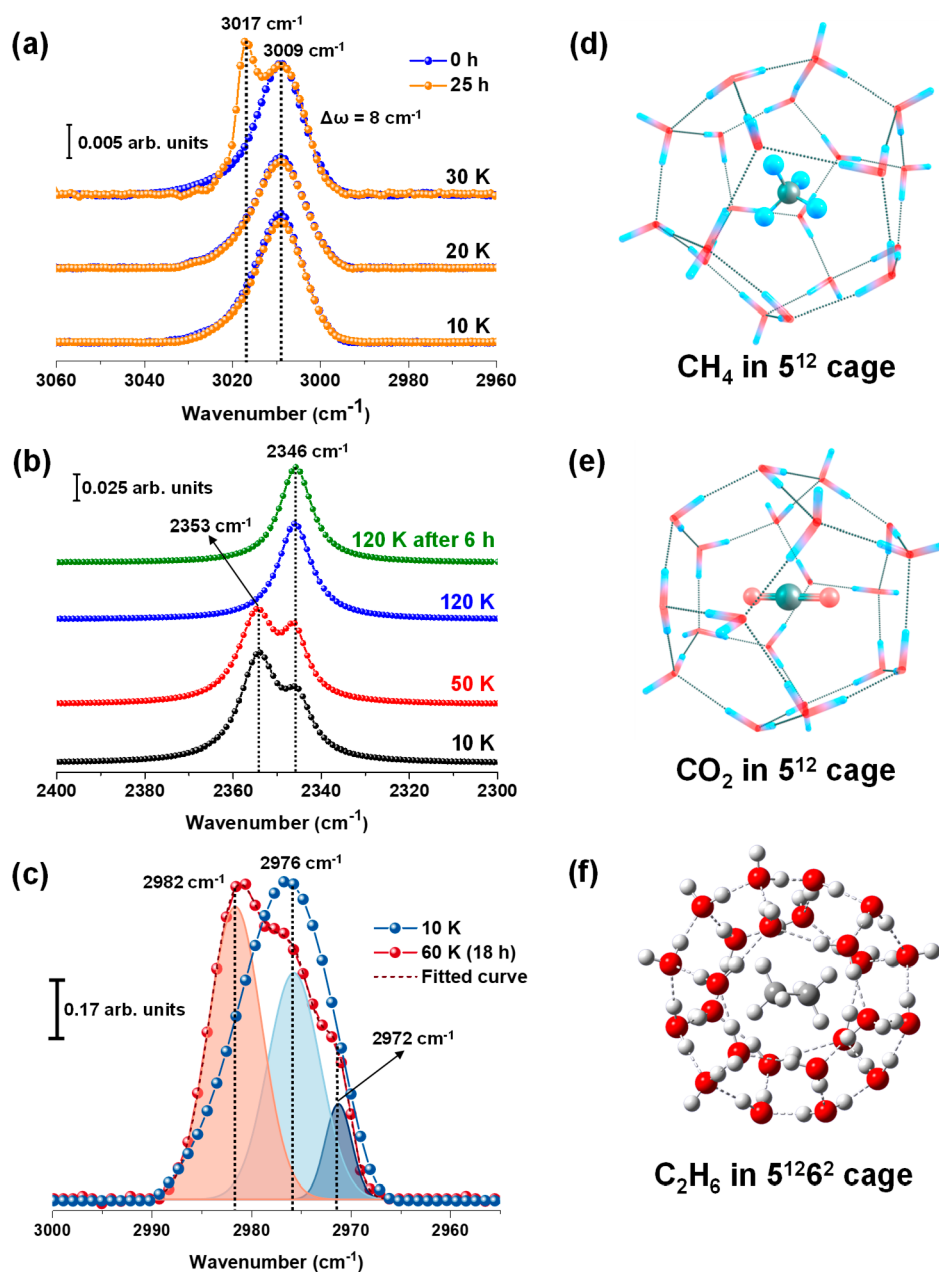


Figure 2. Formation of CHs is studied by RAIR spectroscopy and quantum chemical calculations. RAIR spectra of 300 MLs (1:1) codeposited ice systems, namely, (a) $\text{CH}_4 + \text{H}_2\text{O}$, (b) $\text{CO}_2 + \text{H}_2\text{O}$, and (c) $\text{C}_2\text{H}_6 + \text{H}_2\text{O}$ at different temperatures and annealing times, as indicated. Here, only the C–H and C=O antisymmetric stretching regions are shown for hydrocarbons and CO_2 , respectively. DFT-optimized structures of hydrate cages are shown for (d) CH_4 hydrate, (e) CO_2 hydrate, and (f) C_2H_6 hydrate. Adapted with permission from ref 1. Copyright 2019 the authors. Published by the National Academy of Sciences under Creative Commons Attribution-NonCommercial-NoDerivatives License 4.0 (CC BY-NC-ND) and adapted with permission from ref 43. Copyright 2022 American Chemical Society.

and the MS intensities of these species were utilized to determine the molecular ratio. The mixed ice was heated at 2 K min^{-1} to the desired temperature. RAIR spectra were obtained to monitor CH formation. Identical experimental conditions were maintained throughout the spectral measurement.

3. CLATHRATE HYDRATES UNDER INTERSTELLAR CONDITIONS

3.1. IR Spectroscopic Evidence

We started our quest for CHs in the ISM with CH_4 hydrate, the most common gas hydrate found on earth. At first, 300

MLs of 1:1 CH_4 and water were codeposited at 10 K. Time-dependent RAIR spectra were recorded in the C–H antisymmetric stretching region of CH_4 at 10, 20, and 30 K for different annealing times (0 and 25 h) as shown in Figure 2a. The spectra showed an IR feature of solid CH_4 at 3009 cm^{-1} , which remained constant at 10 and 20 K even after 25 h.¹ However, a new peak at 3017 cm^{-1} appeared after 25 h of annealing at 30 K, which was blue-shifted in comparison to the spectral band for solid CH_4 (3009 cm^{-1}).¹ This new peak (3017 cm^{-1}) was assigned to CH_4 hydrate, and the experimental blue shift of 8 cm^{-1} was due to the entrapment of CH_4 in the hydrate cage.¹ Previous study⁴⁰ had suggested that the trapped guest molecules in CH cages have more

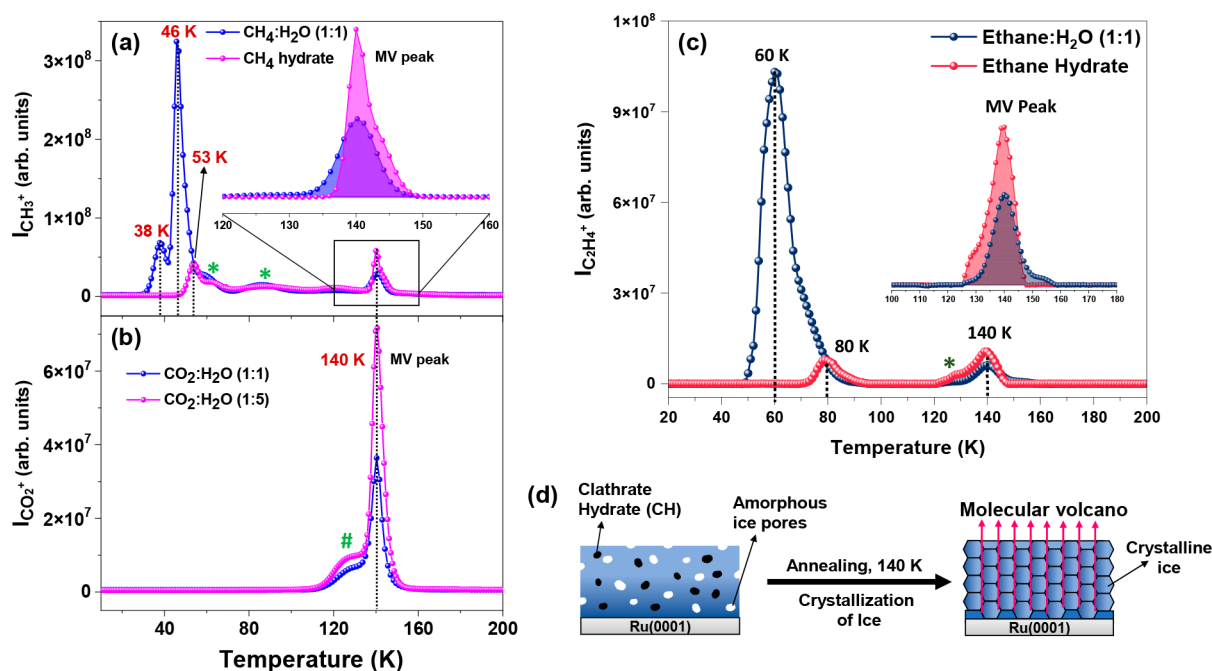


Figure 3. TPD mass spectra of 300 MLs of codeposited ice systems at different ratios (heating rate = 30 K min⁻¹). Here, the intensities of CH₃⁺ ($m/z = 15$), CO₂⁺ ($m/z = 44$), and C₂H₄⁺ ($m/z = 28$) are plotted with the substrate temperature. (a) Desorption of CH₄ before (blue trace) and after hydrate formation (magenta trace). (b) Desorption of CO₂ after hydrate formation at different ratios, as indicated. (c) Desorption of C₂H₆ before (dark-blue trace) and after (red trace) hydrate formation. (d) Schematic representation of molecular volcano (MV) upon crystallization of ice. MV peaks are shown in the insets. Adapted with permission from ref 1. Copyright 2019 the authors. Published by the National Academy of Sciences under a Creative Commons Attribution-NonCommercial-NoDerivatives License 4.0 (CC BY-NC-ND) and adapted with permission from ref 43. Copyright 2022 American Chemical Society.

vibrational freedom and behave like gaseous species; therefore, their vibrational frequency stays in between their gaseous- and condensed-phase frequencies. Another study⁴¹ also showed a blue-shifted IR feature due to CH₄ trapped in a hydrate cage. The prolonged annealing (25 h) at 30 K, near the desorption temperature of CH₄, was crucial to forming the hydrate cage.¹ Primarily due to the application of UHV at these temperatures, CH₄ molecules gained enhanced mobility, which led to the mixing of CH₄ and codeposited water, which results in enhanced interaction and CH₄ insertion into the hydrate cages.¹ A time-dependent RAIR study of pure condensed CH₄ in the absence of water at 25 K did not show the peak at 3017 cm⁻¹, which confirmed its assignment to CH₄ hydrate. In addition, quantum chemical calculations using density functional theory (DFT) also confirmed the formation of CH₄ hydrate. It revealed the preferential formation of stable, small 5¹² cages (Figure 2d) under the simulated condition.¹ The calculated vibrational shift with the formation of CHs nearly matches the experimentally obtained spectral shift (8 cm⁻¹). A microsecond molecular dynamics (MD) simulation study⁴² of CH₄ hydrate nucleation predicted the preferential formation of smaller 5¹² cages during the initial stages of nucleation, which supports our result.

The existence of CHs in ISM was further supported by the experimental evidence of two other hydrates, namely, CO₂¹ and C₂H₆ hydrates.⁴³ An earlier report²⁸ suggested that CO₂ hydrate can be formed at 1.33 × 10⁻⁶ mbar and 120 K. Figure 2b shows the RAIR spectra of 300 MLs of a CO₂:H₂O (1:5) codeposited mixture in the C=O antisymmetric stretching region. The peak at 2346 cm⁻¹ was attributed to CO₂ hydrate, entrapped in the 5¹² cage as suggested by the DFT calculations (Figure 2e).¹ The other peak at 2353 cm⁻¹ was due to the

remaining untrapped solid CO₂, which exists outside the hydrate cages in the amorphous ice matrix.¹ The 2346 cm⁻¹ peak was the characteristic feature of CO₂ hydrate as reported before.²⁸ The gradual decrease in intensity for the 2353 cm⁻¹ peak and the simultaneous emergence of the 2346 cm⁻¹ peak with temperature suggested that annealing helps in better mixing of ice and CO₂, which favors the formation of CO₂ hydrate. The results suggested that CO₂ hydrate can be formed at 10 K, and it is quite stable at 120 K for 6 h. This is attributed to the stronger interaction of CO₂ with water than with CH₄, although both are weak.^{1,44} The formation of C₂H₆ hydrate in ISM was also explored.⁴³ As per an earlier study,²⁵ C₂H₆ hydrate can be formed at 10⁻⁷ mbar and 90 K but only in the presence of oxirane, which helped in the nucleation of ethane-oxirane mixed hydrate. Figure 2c shows the RAIR spectra of a 300 MLs C₂H₆:H₂O (1:1) codeposited mixture in the C–H antisymmetric stretching region at different temperatures.⁴³ Three distinct peaks appeared at 60 K, positioned at 2972, 2976, and 2982 cm⁻¹ corresponding to the crystalline, amorphous, and CH forms of C₂H₆, respectively.⁴³ The 2982 cm⁻¹ peak is the characteristic IR feature of C₂H₆ hydrate as observed in earlier reports.^{25,45} Again, the blue-shifted nature of the 2982 cm⁻¹ peak as compared to the amorphous and crystalline IR features of C₂H₆ indicates its assignment to C₂H₆ hydrate. A comparison of DFT-calculated vibrational and experimental shifts suggested that C₂H₆ is trapped in the 5¹²6² cage as shown in Figure 2f.⁴³

3.2. Mass Spectrometric Evidence

Temperature-programmed desorption-mass spectrometry (TPD-MS) also supported the formation of CHs in ISM. TPD-MS is an MS-based analytical technique routinely utilized in surface science and laboratory astrochemical experiments.

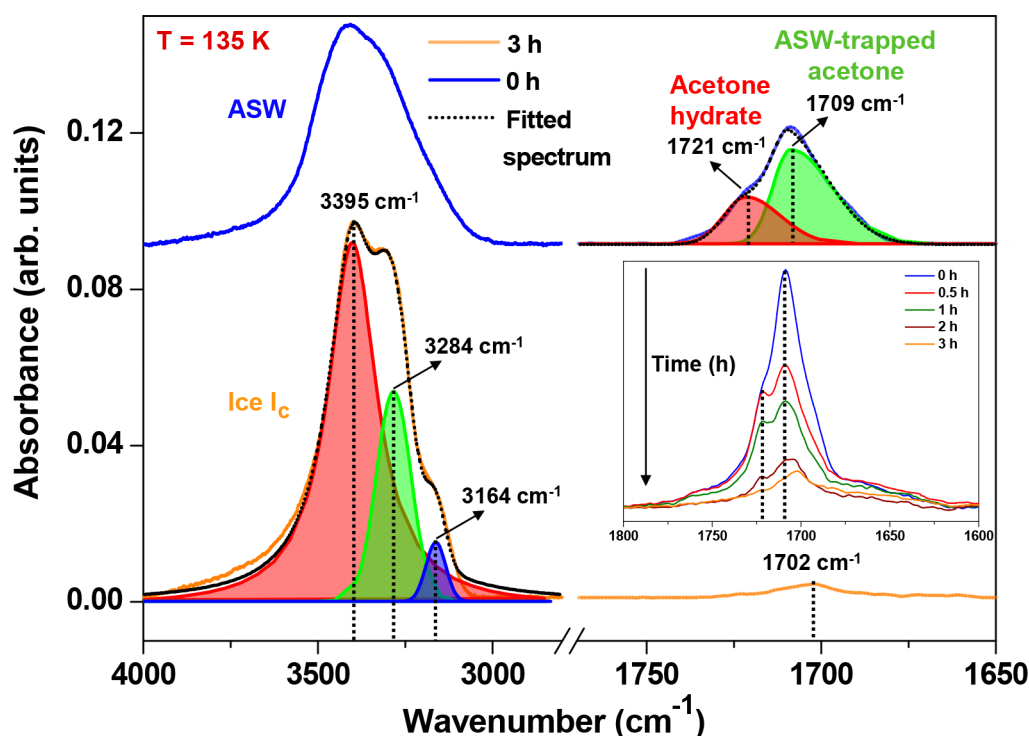


Figure 4. RAIR spectra of 300 MLs of acetone:H₂O (1:1) in the O–H and C=O stretching regions at 135 K. The inset shows the change in the C=O stretching band due to the dissociation of acetone hydrate with time. Here, the blue and orange traces are attributed to amorphous solid water (ASW) and cubic crystalline ice (ice I_c). The spectral change of the O–H band is due to ice crystallization, and different features were resolved upon deconvolution. Adapted with permission from ref 2. Copyright 2020 American Chemical Society.

Here, the continuous desorption of adsorbed species from the substrate upon thermal stimulation is analyzed by a mass spectrometer, and the resultant mass intensities are plotted as a function of the substrate temperature. Porous amorphous ice can entrap guest molecules, which are released during the crystallization of ice at 140 K due to the collapse of these pores.⁴⁶ This results in an abrupt release of the trapped species, which produces a “molecular volcano (MV)”.⁴⁶ Figure 3a represents the comparative TPD spectra before and after the formation of CH₄ hydrate, which were monitored using the intensity of the CH₃⁺ peak ($m/z = 15$).¹ CH₄ hydrate was formed by annealing a codeposited mixture at 30 K for 25 h as mentioned before. The other peaks at 38 and 46 K correspond to multilayer CH₄ and CH₄ trapped in the ASW pores, respectively. The intensity of the MV peak before the formation of the hydrate is due to the trapped CH₄ in ASW, whereas the intensity of the MV peak was enhanced upon the formation of the hydrate due to the simultaneous release of trapped CH₄ from ASW pores as well as from the hydrate cages (Figure 3a).¹ Note that the amounts of gases deposited are the same in both cases. The slight distortion in the MV peak is attributed to the modification of ASW pores due to CH formation (Figure 3a). Figure 3b shows the TPD spectra of 300 MLs of CO₂ + H₂O at two ratios, 1:1 and 1:5, and they were annealed at 120 K for the complete formation of CO₂ hydrate.¹ Then the samples were cooled back to 10 K, and TPD spectra were recorded. The peak at 140 K corresponds to the MV of CO₂, and its intensity increased as the ratio of CO₂ to H₂O was changed from 1:1 to 1:5. Experiments suggested that the extent of formation of CO₂ hydrate was greater for the diluted water and CO₂ mixture, and it agreed well with the IR spectral interpretation.^{1,44}

Figure 3c shows the TPD profiles for C₂H₆ hydrate before and after formation.⁴³ Two sets of TPD-MS experiments were performed; in the first, we deposited 300 MLs of an C₂H₆:H₂O (1:1) ice mixture at 10 K and heated it to 200 K at a ramping rate of 30 K min⁻¹. The desorption of C₂H₆ was monitored by the intensity of the C₂H₄⁺ peak ($m/z = 28$). The peaks at 60 and 140 K were attributed to the desorption of multilayer C₂H₆ from ASW pores and the MV peak, respectively.⁴³ In the second experiment, a C₂H₆:H₂O (1:1) ice mixture was annealed at 60 K for 18 h to create C₂H₆ hydrate. After the hydrate was formed, the sample was cooled to 10 K and the TPD spectrum was recorded (red trace), which showed two peaks at 80 and 140 K. The peak at 80 K was assigned to the desorption of trapped C₂H₆ (amorphous or crystalline) from the ASW matrix. The peak was shifted from 60 to 80 K primarily due to the formation of CH as well as a more compact ice network as a result of prolonged annealing.⁴³ The MV peak of C₂H₆ hydrate showed a higher intensity compared to the MV peak before hydrate formation. The enhanced intensity of the MV peak for the hydrate was due to the release of trapped C₂H₆ from the ASW pores and the dissociation of the CH cage, as explained before. Note that the peak marked by an asterisk around 125 K was due to the desorption of C₂H₆ due to the predissociation of hydrate cages.⁴³

4. TRANSFORMATIONS OF CLATHRATE HYDRATES

4.1. Formation of Cubic Ice (Ice I_c) from CH

The dissociation behavior⁴⁷ of CHs is also important to understand since it leads to different crystalline phases of ice. An earlier study⁴⁸ suggested that emptying neon from its hydrate cages led to the formation of ice XVI, a new crystalline phase of ice. The dissociation of CO₂ hydrates led to cubic ice

(ice I_c).⁴⁹ In our study,² we showed that acetone hydrates could be prepared by codepositing acetone:H₂O (1:1) mixtures and annealing them to 135 K. However, keeping acetone hydrate at 135 K for 3 h led to its dissociation, which resulted in ice I_c .² Figure 4 shows the RAIR spectra of the codeposited film at 135 K (blue trace; 0 h) and after 3 h (orange trace; 3 h).² The inset shows the C=O stretching band, and at 0 h, it shows two features at 1721 and 1709 cm⁻¹ which were attributed to acetone hydrate^{50,51} and ASW-trapped acetone,⁵² respectively. The peak intensity was reduced with time and resulted in a peak at 1702 cm⁻¹, which was assigned to a dilute mixture of acetone and water (1:20). The profound change in the O–H stretching band with time indicates the change in the overall structure of ice due to the dissociation of acetone hydrate.² In Figure 4, the broad O–H stretching band (blue trace) is a characteristic feature of ASW, which eventually became sharp and developed three shoulder features after 3 h (orange trace). Ice crystallization is generally associated with the splitting and sharpening of the O–H stretching band, and it was deconvoluted to three distinct features at 3164, 3284, and 3395 cm⁻¹, corresponding to the ν_1 in-phase band, the ν_3 TO band, and the overlapped ν_3 LO and ν_1 out-of-phase bands of ice I_c .⁵³ Isotopic experiments with an acetone:D₂O (1:1) system also led to the formation of cubic D₂O ice due to the dissociation of acetone hydrate (not shown).² Note that, in similar studies at 130 K, the ice I_c conversion took 9 h, whereas the ice I_c was not observed at 120 K, even after 48 h. The thermal motion of acetone molecules is likely to be responsible for the formation of acetone hydrate and subsequently ice I_c .² In a similar study, the dissociation of acetaldehyde hydrate leads to the formation of ice I_c .⁵⁴

We have also provided more direct structural evidence to support the claim of forming ice I_c via hydrate dissociation.² Figure 5 shows the time-dependent reflection high-energy electron diffraction (RHEED) images of acetone:H₂O (1:1) at different temperatures.² In Figure 5a, the RHEED image does not show any pattern, indicating the amorphous nature of the mixture. However, several diffraction rings were observed after 5 h (Figure 5b).² Here, most of the acetone molecules desorb from the mixture, as indicated by the IR spectra. Note that these diffraction patterns originate from the ice I_c and match the earlier diffraction studies of ice I_c .^{55,56} Time-dependent RHEED studies at 130 K showed an ice I_c pattern after 12 h (Figure 5d). However, the diffraction patterns were not observed at 120 K, even after 24 h (Figure 5e,f). These observations support the RAIR spectral interpretation, which suggests that ice I_c was formed only through the dissociation of acetone hydrate.²

4.2. Formation of Hexagonal Ice (Ice I_h) from CH

Among several polymorphs of ice, hexagonal ice (ice I_h) is the most common, and it occurs naturally on earth. However, the formation of ice I_h from CH precursors was not studied. We found that formaldehyde hydrate dissociated to form ice I_h under UHV at 130–135 K.³ Figure 6a,b shows the time-dependent RAIR spectra of the codeposited formaldehyde:H₂O (1:1) film at 135 K in the C=O and O–H stretching regions, respectively. The IR feature at 1733 cm⁻¹ is attributed to the C=O stretching band of formaldehyde hydrate (Figure 6a).³ This assignment was performed by comparing formaldehyde vapor (1746 cm⁻¹) and condensed phase (1723 cm⁻¹) frequencies. The hydrate phase frequencies fall in

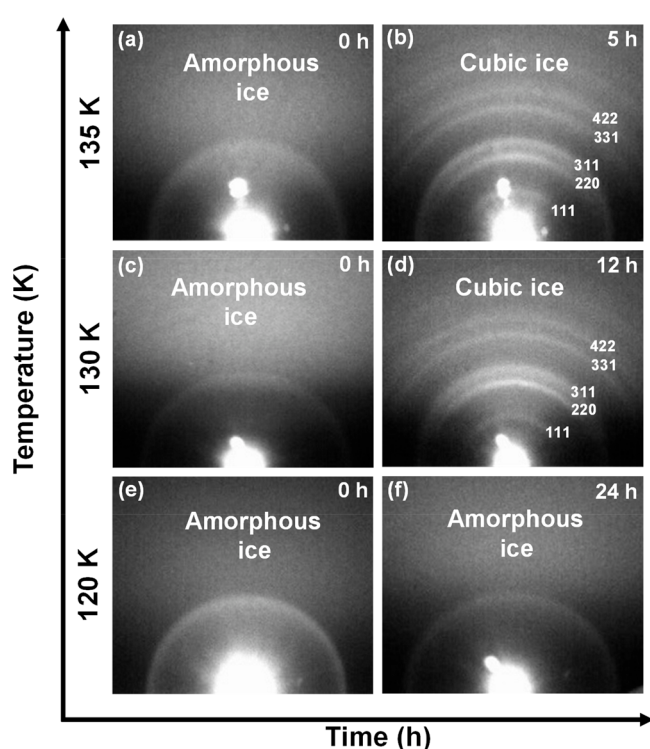


Figure 5. Time-dependent RHEED images of 300 MLs of acetone:H₂O (1:1) at 120, 130, and 135 K and different annealing times, as indicated. After codeposition, the mixtures were annealed at 2 K min⁻¹ to reach the required temperatures. Adapted with permission from ref 2. Copyright 2020 American Chemical Society.

between them.³ Besides, the O–H stretching region showed a profound change after 5 h with the disappearance of the formaldehyde hydrate IR peak. This O–H stretching band (blue trace) is the characteristic feature of ice I_h as confirmed by comparing pure crystalline ice I_h spectra, recorded independently. The control study also suggested that water by itself cannot form ice I_h at 135 K in the absence of formaldehyde hydrate since its usual crystallization temperature is 150–155 K under UHV. The existence of formaldehyde and water in space suggests the possibility to form hydrates and their subsequent transformation to ice I_h , which constitutes a mechanistic route for its formation in ISM.³

5. STRUCTURAL DYNAMICS OF CLATHRATE HYDRATES

The structural dynamics in CHs are important to study, which reveals that the reorientation of water and the diffusion of guest molecules are the driving forces for these structures. Furthermore, the presence of a second guest species provides extra thermodynamic stability to the hydrate framework, and they are termed binary CHs. THF hydrate is known to be a stabilizer for such binary CHs.⁴ THF being a larger molecule occupies the larger cages ($S^{12}6^4$), whereas the other guest species occupy the smaller ones (S^{12}). Here, we have studied the formation of THF hydrate by codepositing a THF:H₂O mixture (1:5) and annealing it to 130 K.⁴ Figure 7a,b shows the time-dependent spectra of the same system in the asymmetric C–O and O–H stretching regions. The peaks at 1034 and 1053 cm⁻¹ were assigned to THF trapped in different sites of ASW, whereas the other peak at 1074 cm⁻¹ is the characteristic feature of THF hydrate.⁴ Continuous

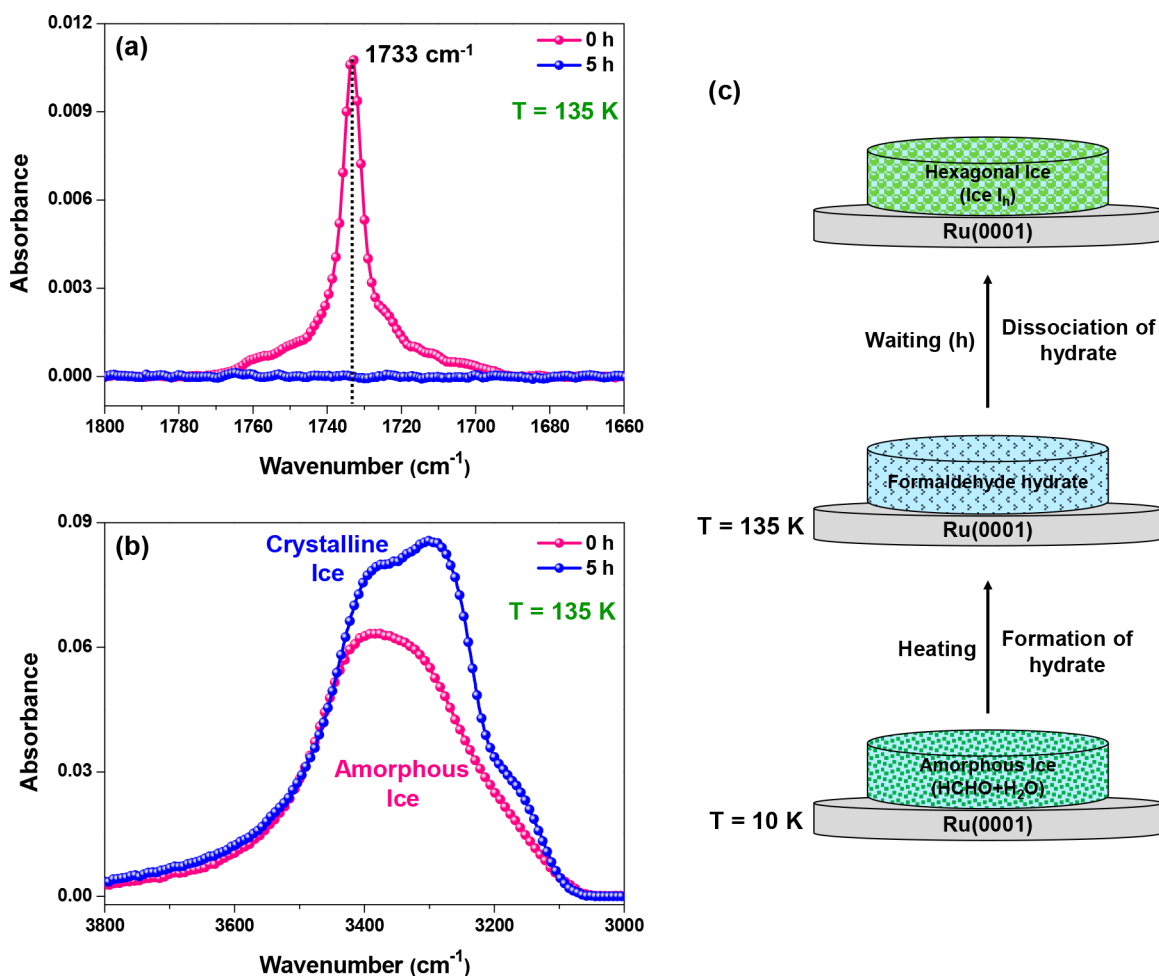


Figure 6. Time-dependent RAIR spectra of 300 MLs of formaldehyde:H₂O (1:1) at 135 K in the (a) C=O and (b) O–H stretching regions. (c) The schematic illustration shows the formation of formaldehyde hydrate and its dissociation, which leads to the formation of hexagonal ice (ice I_h). Adapted with permission from ref 3. Copyright 2021 American Chemical Society.

annealing (6 h) of the system increased the intensity of the THF hydrate peak and decreased the intensity of the other two peaks. The 1074 cm⁻¹ peak serves as a convenient indicator of THF hydrate since it lies well above the IR peak positions of other likely condensed phases of THF. In Figure 7b, the O–H stretching band is also red-shifted with time, which was an indication of ice crystallization. Results suggested that the gradual transformation of THF hydrate also changes the structure of ice from amorphous to crystalline.⁴ Furthermore, the crystallization kinetics suggested that the formation of THF hydrate was a diffusion-controlled process.⁴ In addition, this study has the potential to explore a certain number of binary CHs. To explore this possibility, we conducted a study with a CO₂@(THF + H₂O; 1:5) composite ice film, where a THF + water mixture was sequentially deposited on a predeposited CO₂ film and this system was annealed at 130 K for 6 h.⁵⁷ Figure 7c,d shows the corresponding time-dependent RAIR spectra in the C=O and C–O antisymmetric stretching regions of CO₂ and THF, respectively. The IR peaks at 2352, 2346, and 2340 cm⁻¹ were assigned to CO₂ in the ASW matrix and 5¹² and 5¹²6² cages, respectively.^{1,26,57} Continuous annealing decreased the intensity of the 2346 cm⁻¹ peak and increased that of the 2352 cm⁻¹ peak, whereas the intensity of the 2340 cm⁻¹ peak remained constant. It suggested that CO₂ was transported from 5¹²6² cages to the

ASW matrix and that CO₂ in 5¹² cages remained mostly unperturbed.⁵⁷ In Figure 7c, a new peak arose at 1074 cm⁻¹ while the peaks at 1054 and 1032 cm⁻¹ decreased with time, as shown in Figure 7c,d. The peak at 1074 cm⁻¹ was the characteristic peak for THF hydrate encased in 5¹²6⁴ cages, whereas the peaks at 1054 and 1032 cm⁻¹ were assigned to THF trapped in ASW pores.^{4,27,50} The formation of stable binary THF-CO₂ hydrate is a possibility, which is confirmed by the IR features of individual guest species (2346 and 1074 cm⁻¹ of CO₂ and THF), and computationally optimized structures also supported this observation.⁵⁷ The higher mobility of CO₂ in comparison to THF favors the formation of the CO₂ hydrate, kinetically. However, upon annealing at higher temperatures for a longer time, the formation of THF hydrate is triggered. The larger size of THF makes it a preferred guest over CO₂ in large (5¹²6⁴) cages. This leads to partial dissociation of CO₂ cages and rearrangement of the hydrate structure resulting in the increase in CO₂ in the ASW matrix, as shown schematically in Figure 7e.⁵⁷

From the foregoing, it is evident that several CHs can be formed under UHV if subjected to certain key experimental conditions such as the annealing temperature, time, and stoichiometric ratio. The extreme low-temperature conditions in ISM result in a mass transfer limitation, primarily due to limited natural convection (and mixing of species), which may

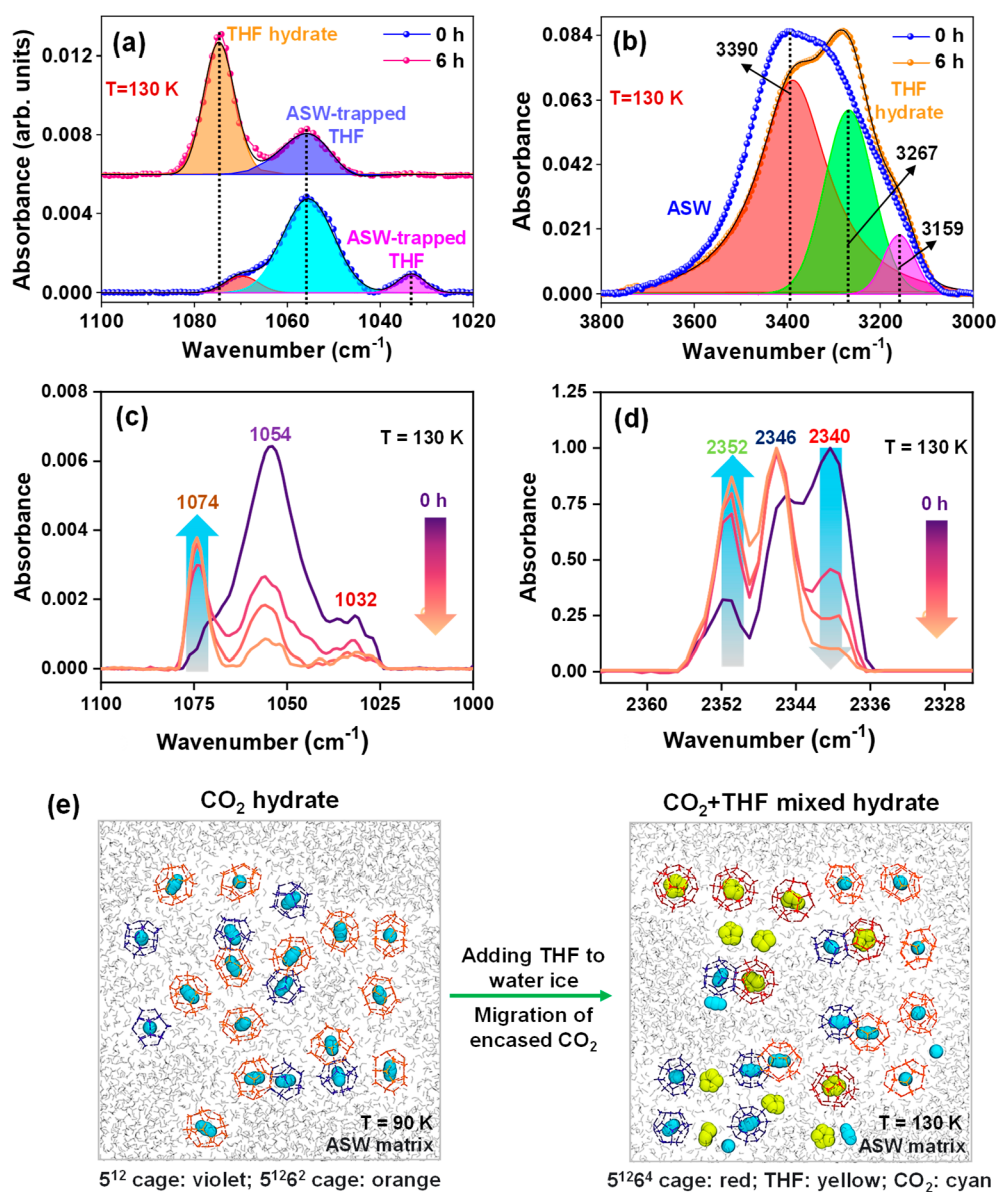


Figure 7. Time-dependent RAIR spectra of 300 MLs of THF:H₂O (1:1) in the (a) asymmetric C–O and (b) O–H stretching regions and of CO₂@(THF + H₂O; 1:5) at 130 K in the (c) asymmetric C–O and (d) C=O antisymmetric stretching regions at 130 K. (e) The schematic illustration shows the formation of the THF-CO₂ hydrate and the migration of CO₂ from 5¹²6² cages to the ASW matrix upon its dissociation by annealing at 130 K. Color code used: 5¹² cage, violet; 5¹²6² cage, orange; 5¹²6⁴ cage, red; THF, yellow; and CO₂, cyan. Adapted with permission from ref 4. Copyright 2019 American Chemical Society and adapted with permission from ref 57. Copyright 2023 American Chemical Society.

hinder the nucleation process of CHs. Achieving sufficient molecular mobility is key to forming the hydrates, which is obtained by prolonged annealing of the system near their respective desorption temperatures, irrespective of the type of guest. As per our understanding based on the experimental results, the mechanism of CH formation involves the solvation or mixing of guest molecules with water molecules as the first step. It is followed by the formation of hydrate cages around the solvated guest molecules in a stochastic manner. On the other hand, the formation of different crystalline forms of ice upon dissociation of hydrate is possibly due to the orientational defects (Bjerrum defects).^{57–59} The guest–host hydrogen bonding causes defects within the water network (host), which again depends on the type of guest molecules present in the hydrate cages. However, these defect-induced structural changes are only partially understood, and computational

studies involving MD simulations on the formation and dissociation behavior of CHs may provide additional insights.

6. PHOTOCHEMICAL EFFECTS ON CLATHRATE HYDRATES

Light irradiation is known to initiate photochemistry in ISM ices, which is suggested to be a path to chemical complexity in space.⁶ These experiments involve single, binary, or multi-component ice mixtures with a range of radiation (MeV electrons/protons to high-energy UV photons).⁶ Upon radiation exposure, water–ice dissociates to produce highly reactive radicals and initiates radical chemistry.⁶ However, high diffusion barriers of radicals in ice present restricted photochemistry.⁶ On the contrary, CHs were shown to act as a host for unique hydrogen transfer reactions involving radicals.^{60,61} Furthermore, the CH cages were demonstrated to store⁶² and

stabilize the free radicals⁶³ under high-pressure conditions. Given this, the photochemistry of CHs would be interesting under UHV and cryogenic conditions, where the guest molecule AB could dissociate to form A and B radicals. Depending on the size and kinetic energy, the fate of these radicals may vary such as recombination, stabilization upon entrapment, movement to the adjacent cage, and reaction with AB, A, or B.^{60–62}

So far, ice photochemical experiments resulted in racemic mixtures of the photolyzed products and not the homochiral form found on earth, which remains an unsolved puzzle in chemistry. The entrapped species in CH cages may interact with radiation asymmetrically to produce either left- or right-handed molecules. The proposed study can shed light on the origin of enantiomeric excess on earth.

7. FUTURE PERSPECTIVES

In this Account, the investigation of different CHs and their several important aspects such as nucleation conditions, mechanism, stability, and transformation to other ice structures are presented in the context of interstellar processes. The results suggested that the temperature and annealing time are crucial parameters in deciding the formation and structural changes of CHs. The key outcome of these studies is that it provides conclusive evidence that several CHs are formed at extremely low pressures and temperatures, conditions analogous to the ISM. This finding may open several possibilities for future explorations. While the formation of CHs of simple molecules such as methane, ethane, and carbon dioxide in interstellar-like environments is already established in the current study, many other guest molecules such as H₂, CO, N₂, O₂, NH₃, and C₂H₂ are known to form CHs, which are also found in space or the ISM along with water in solid form. Therefore, we believe that this Account will provide a direction to investigate several other CHs under suitable conditions. Furthermore, the fate of CHs upon their dissociation could be an exciting area to explore since CHs can transform into different polymorphs of ice, as highlighted in this Account. The nucleation mechanism, stability, and structure of several polymorphs of ice are intriguing. Formation and detailed studies of binary CHs under interstellar-like conditions would be another direction. Our studies have provided an early hint that binary CHs could be formed in the presence of appropriate stabilizers such as THF. In addition, these binary CHs can be utilized as precursors for interguest chemical interactions under extreme conditions of ISM such as UV and particle impact.

Apart from these possibilities, the ultimate goal of the astrochemistry community is to understand the origin of life. Understanding the chemical evolution of simple molecules to COMs has been a long-standing question. CHs can be an ideal precursor to trap several simple guest species that can undergo chemical reactions. The presence of cosmic radiation could be the driving force in such exotic environments. More experimental studies in this direction are necessary for a complete understanding of the phenomena involved. The utilization of the direct structural interpretation of CHs through extensive diffraction data^{2,64} under such extreme conditions will provide important insights. There is also a need to understand the dynamics of the formation of CHs in UHV starting from ice mixtures, which will require detailed computational studies. Despite these challenges, we hope that the present investigations have provided new insights into

the fascinating area of CHs and suggest exciting new directions for the future.

AUTHOR INFORMATION

Corresponding Authors

Rajnish Kumar – Department of Chemical Engineering, Indian Institute of Technology Madras, Chennai 600036, India; orcid.org/0000-0002-4172-2638; Email: rajnish@iitm.ac.in

Thalappil Pradeep – Department of Chemistry, DST Unit of Nanoscience (DST UNS) and Thematic Unit of Excellence (TUE), Indian Institute of Technology Madras, Chennai 600036, India; orcid.org/0000-0003-3174-534X; Email: pradeep@iitm.ac.in

Authors

Jyotirmoy Ghosh – Department of Chemistry, DST Unit of Nanoscience (DST UNS) and Thematic Unit of Excellence (TUE), Indian Institute of Technology Madras, Chennai 600036, India

Gaurav Vishwakarma – Department of Chemistry, DST Unit of Nanoscience (DST UNS) and Thematic Unit of Excellence (TUE), Indian Institute of Technology Madras, Chennai 600036, India

Complete contact information is available at: <https://pubs.acs.org/10.1021/acs.accounts.3c00317>

Notes

The authors declare no competing financial interest.

Biographies

Jyotirmoy Ghosh earned his Ph.D. in physical chemistry from the Indian Institute of Technology Madras in 2020 under the guidance of Prof. Thalappil Pradeep. He is currently a postdoctoral research associate at Purdue University, USA. His Ph.D. research has been focused on the investigations of clathrate hydrates and ice systems of interstellar relevance under UHV and cryogenic conditions.

Gaurav Vishwakarma is a Ph.D. student at the Indian Institute of Technology Madras under the guidance of Prof. Thalappil Pradeep. His research focuses on the investigations of clathrate hydrates and ice systems under UHV and cryogenic conditions.

Rajnish Kumar is a professor at the Indian Institute of Technology Madras. His research interests are in the formation of gas hydrates and their applications in energy storage, transportation, CO₂ capture, water treatment, and desalination.

Thalappil Pradeep is an institute professor and the Deepak Parekh Institute Chair Professor at the Indian Institute of Technology Madras. He works on nanomaterials, water purification, and the chemistry of molecular solids such as ice. He has developed state-of-the-art instrumentation for such studies.

ACKNOWLEDGMENTS

J.G. and G.V. thank the University Grants Commission (UGC) and IIT Madras for their research fellowships. The authors thank the Science and Engineering Research Board (SERB) and the Department of Science and Technology (DST), Government of India, for research funding. T.P. acknowledges funding from the Centre of Excellence on Molecular Materials and Functions under the Institution of Eminence scheme of IIT Madras.

REFERENCES

- (1) Ghosh, J.; Methikkalam, R. R. J.; Bhui, R. G.; Ragupathy, G.; Choudhary, N.; Kumar, R.; Pradeep, T. Clathrate Hydrates in Interstellar Environment. *Proc. Natl. Acad. Sci. U. S. A.* **2019**, *116*, 1526–1531.
- (2) Ghosh, J.; Bhui, R. G.; Vishwakarma, G.; Pradeep, T. Formation of Cubic Ice via Clathrate Hydrate, Prepared in Ultrahigh Vacuum under Cryogenic Conditions. *J. Phys. Chem. Lett.* **2020**, *11*, 26–32.
- (3) Ghosh, J.; Vishwakarma, G.; Das, S.; Pradeep, T. Facile Crystallization of Ice I_h via Formaldehyde Hydrate in Ultrahigh Vacuum under Cryogenic Conditions. *J. Phys. Chem. C* **2021**, *125*, 4532–4539.
- (4) Ghosh, J.; Bhui, R. G.; Ragupathy, G.; Pradeep, T. Spontaneous Formation of Tetrahydrofuran Hydrate in Ultrahigh Vacuum. *J. Phys. Chem. C* **2019**, *123*, 16300–16307.
- (5) Herbst, E. The Chemistry of Interstellar Space. *Chem. Soc. Rev.* **2001**, *30*, 168–176.
- (6) Öberg, K. I. Photochemistry and Astrochemistry: Photochemical Pathways to Interstellar Complex Organic Molecules. *Chem. Rev.* **2016**, *116*, 9631–9663.
- (7) McGuire, B. A. 2021 Census of Interstellar, Circumstellar, Extragalactic, Protoplanetary Disk, and Exoplanetary Molecules. *Astrophys. J. Suppl. Ser.* **2022**, *259*, 30.
- (8) Gibb, E. L.; Whittet, D. C. B.; Boogert, A. C. A.; Tielens, A. G. G. M. Interstellar Ice: The Infrared Space Observatory Legacy. *Astrophys. J. Suppl. Ser.* **2004**, *151*, 35.
- (9) Oberg, K. I.; Boogert, A. C. A.; Pontoppidan, K. M.; van den Broek, S.; van Dishoeck, E. F.; Bottinelli, S.; Blake, G. A.; Evans, N. J. The Spitzer Ice Legacy: Ice Evolution from Cores to Protostars. *Astrophys. J.* **2011**, *740*, 109.
- (10) Boogert, A. C. A.; Gerakines, P. A.; Whittet, D. C. B. Observations of the Icy Universe. *Annu. Rev. Astron. Astrophys.* **2015**, *53*, 541–581.
- (11) Sloan, E. D. Fundamental Principles and Applications of Natural Gas Hydrates. *Nature* **2003**, *426*, 353–359.
- (12) Ripmeester, J. A.; Tse, J. S.; Ratcliffe, C. L.; Powell, B. M. A New Clathrate Hydrate Structure. *Nature* **1987**, *325*, 135–136.
- (13) Makogon, Y. F. A Gas Hydrate Formation in the Gas Saturated Layers under Low Temperature. *Gas Ind.* **1965**, *5*, 14–15.
- (14) Chong, Z. R.; Yang, S. H. B.; Babu, P.; Linga, P.; Li, X.-S. Review of Natural Gas Hydrates as an Energy Resource: Prospects and Challenges. *Appl. Energy* **2016**, *162*, 1633–1652.
- (15) Khurana, M.; Yin, Z.; Linga, P. A Review of Clathrate Hydrate Nucleation. *ACS Sustain. Chem. Eng.* **2017**, *5*, 11176–11203.
- (16) Yin, Z.; Zheng, J.; Kim, H.; Seo, Y.; Linga, P. Hydrates for Cold Energy Storage and Transport: A Review. *Adv. Appl. Energy* **2021**, *2*, No. 100022.
- (17) Rufford, T. E.; Smart, S.; Watson, G. C. Y.; Graham, B. F.; Boxall, J.; Diniz da Costa, J. C.; May, E. F. The Removal of CO₂ and N₂ from Natural Gas: A Review of Conventional and Emerging Process Technologies. *J. Pet. Sci. Eng.* **2012**, *94–95*, 123–154.
- (18) Hughes, T. J.; Honari, A.; Graham, B. F.; Chauhan, A. S.; Johns, M. L.; May, E. F. CO₂ Sequestration for Enhanced Gas Recovery: New Measurements of Supercritical CO₂–CH₄ Dispersion in Porous Media and a Review of Recent Research. *Int. J. Greenh. Gas Control* **2012**, *9*, 457–468.
- (19) Kang, K. C.; Linga, P.; Park, K.; Choi, S.-J.; Lee, J. D. Seawater Desalination by Gas Hydrate Process and Removal Characteristics of Dissolved Ions (Na⁺, K⁺, Mg²⁺, Ca²⁺, B³⁺, Cl⁻, SO₄²⁻). *Desalination* **2014**, *353*, 84–90.
- (20) Hassanpouryouzband, A.; Joonaki, E.; Farahani, M. V.; Takeya, S.; Ruppel, C.; Yang, J.; English, N. J.; Schicks, J. M.; Edlmann, K.; Mehrabian, H.; Aman, Z. M.; Tohidi, B. Gas Hydrates in Sustainable Chemistry. *Chem. Soc. Rev.* **2020**, *49*, 5225–5309.
- (21) Miller, S. L. The Occurrence of Gas Hydrates in the Solar System*. *Proc. Natl. Acad. Sci. U. S. A.* **1961**, *47*, 1798–1808.
- (22) Miller, S. L.; Smythe, W. D. Carbon Dioxide Clathrate in the Martian Ice Cap. *Science* **1970**, *170*, 531–533.
- (23) Tobie, G.; Lunine, J. I.; Sotin, C. Episodic Outgassing as the Origin of Atmospheric Methane on Titan. *Nature* **2006**, *440*, 61–64.
- (24) Bertie, J. E.; Devlin, J. P. Infrared Spectroscopic Proof of the Formation of the Structure I Hydrate of Oxirane from Annealed Low-temperature Condensate. *J. Chem. Phys.* **1983**, *78*, 6340–6341.
- (25) Richardson, H. H.; Wooldridge, P. J.; Devlin, J. P. FT-IR Spectra of Vacuum Deposited Clathrate Hydrates of Oxirane H₂S, THF, and Ethane. *J. Chem. Phys.* **1985**, *83*, 4387–4394.
- (26) Fleyfel, F.; Devlin, J. P. FT-IR Spectra of 90 K Films of Simple, Mixed, and Double Clathrate Hydrates of Trimethylene Oxide, Methyl Chloride, Carbon Dioxide, Tetrahydrofuran, and Ethylene Oxide Containing Decoupled D₂O. *J. Phys. Chem.* **1988**, *92*, 631–635.
- (27) Fleyfel, F.; Devlin, J. P. Carbon Dioxide Clathrate Hydrate Epitaxial Growth: Spectroscopic Evidence for Formation of the Simple Type-II Carbon Dioxide Hydrate. *J. Phys. Chem.* **1991**, *95*, 3811–3815.
- (28) Blake, D.; Allamandola, L.; Sandford, S.; Hudgins, D.; Freund, F. Clathrate Hydrate Formation in Amorphous Cometary Ice Analogs in Vacuo. *Science* **1991**, *254*, 548–551.
- (29) Hernandez, J.; Uras, N.; Devlin, J. P. Coated Ice Nanocrystals from Water–Adsorbate Vapor Mixtures: Formation of Ether–CO₂ Clathrate Hydrate Nanocrystals at 120 K. *J. Phys. Chem. B* **1998**, *102*, 4526–4535.
- (30) Delzeit, L.; Devlin, J. P.; Buch, V. Structural Relaxation Rates near the Ice Surface: Basis for Separation of the Surface and Subsurface Spectra. *J. Chem. Phys.* **1997**, *107*, 3726–3729.
- (31) Hallbrucker, A. A Clathrate Hydrate of Nitric Oxide. *Angew. Chem., Int. Ed. Engl.* **1994**, *33*, 691–693.
- (32) Mayer, E.; Hallbrucker, A. Unexpectedly Stable Nitrogen and Oxygen Clathrate Hydrates from Vapour Deposited Amorphous Solid Water. *J. Chem. Soc. Chem. Commun.* **1989**, No. 12, 749–751.
- (33) Hallbrucker, A.; Mayer, E. Unexpectedly Stable Nitrogen, Oxygen, Carbon Monoxide and Argon Clathrate Hydrates from Vapour-Deposited Amorphous Solid Water: An X-Ray and Two-Step Differential Scanning Calorimetry Study. *J. Chem. Soc. Faraday Trans.* **1990**, *86*, 3785–3792.
- (34) Bag, S.; Bhui, R. G.; Methikkalam, R. R. J.; Pradeep, T.; Kephart, L.; Walker, J.; Kuchta, K.; Martin, D.; Wei, J. Development of Ultralow Energy (1–10 eV) Ion Scattering Spectrometry Coupled with Reflection Absorption Infrared Spectroscopy and Temperature Programmed Desorption for the Investigation of Molecular Solids. *Rev. Sci. Instrum.* **2014**, *85*, No. 014103.
- (35) Ghosh, J.; Hariharan, A. K.; Bhui, R. G.; Methikkalam, R. R. J.; Pradeep, T. Propane and Propane–Water Interactions: A Study at Cryogenic Temperatures. *Phys. Chem. Chem. Phys.* **2018**, *20*, 1838–1847.
- (36) Methikkalam, R. R. J.; Bhui, R. G.; Ghosh, J.; Sivaraman, B.; Pradeep, T. Interaction of Acetonitrile with Alcohols at Cryogenic Temperatures. *J. Phys. Chem. C* **2017**, *121*, 2822–2835.
- (37) Methikkalam, R. R. J.; Ghosh, J.; Bhui, R. G.; Bag, S.; Ragupathy, G.; Pradeep, T. Iron Assisted Formation of CO₂ over Condensed CO and Its Relevance to Interstellar Chemistry. *Phys. Chem. Chem. Phys.* **2020**, *22*, 8491–8498.
- (38) Vishwakarma, G.; Ghosh, J.; Pradeep, T. Desorption-Induced Evolution of Cubic and Hexagonal Ices in an Ultrahigh Vacuum and Cryogenic Temperatures. *Phys. Chem. Chem. Phys.* **2021**, *23*, 24052–24060.
- (39) Moon, E.-S.; Kang, H.; Oba, Y.; Watanabe, N.; Kouchi, A. Direct Evidence for Ammonium Ion Formation in Ice Through Ultraviolet-Induced Acid–Base Reaction of NH₃ With H₃O⁺. *Astrophys. J.* **2010**, *713*, 906.
- (40) Buch, V.; Devlin, J. P.; Monreal, I. A.; Jagoda-Cwiklik, B.; Uras-Aytemiz, N.; Cwiklik, L. Clathrate Hydrates with Hydrogen-Bonding Guests. *Phys. Chem. Chem. Phys.* **2009**, *11*, 10245–10265.
- (41) Dartois, E.; Deboffle, D.; Bouzid, M. Methane Clathrate Hydrate Infrared Spectrum - II. Near-Infrared Overtones, Combination Modes and Cages Assignments. *Astron. Astrophys.* **2010**, *514*, A49.

- (42) Walsh, M. R.; Koh, C. A.; Sloan, E. D.; Sum, A. K.; Wu, D. T. Microsecond Simulations of Spontaneous Methane Hydrate Nucleation and Growth. *Science* **2009**, *326*, 1095–1098.
- (43) Malla, B. K.; Vishwakarma, G.; Chowdhury, S.; Selvarajan, P.; Pradeep, T. Formation of Ethane Clathrate Hydrate in Ultrahigh Vacuum by Thermal Annealing. *J. Phys. Chem. C* **2022**, *126*, 17983–17989.
- (44) Ghosh, J.; Methikkalam, R. R. J.; Bhuin, R. G.; Ragupathy, G.; Choudhary, N.; Kumar, R.; Pradeep, T. Reply to Choukroun et al.: IR and TPD Data Suggest the Formation of Clathrate Hydrates in Laboratory Experiments Simulating ISM. *Proc. Natl. Acad. Sci. U. S. A.* **2019**, *116*, 14409–14410.
- (45) Dartois, E.; Langlet, F. Ethane Clathrate Hydrate Infrared Signatures for Solar System Remote Sensing. *Icarus* **2021**, *357*, No. 114255.
- (46) Smith, R. S.; Petrik, N. G.; Kimmel, G. A.; Kay, B. D. Thermal and Nonthermal Physicochemical Processes in Nanoscale Films of Amorphous Solid Water. *Acc. Chem. Res.* **2012**, *45*, 33–42.
- (47) Takeya, S.; Ripmeester, J. A. Dissociation Behavior of Clathrate Hydrates to Ice and Dependence on Guest Molecules. *Angew. Chem., Int. Ed.* **2008**, *47*, 1276–1279.
- (48) Falenty, A.; Hansen, T. C.; Kuhs, W. F. Formation and Properties of Ice XVI Obtained by Emptying a Type SII Clathrate Hydrate. *Nature* **2014**, *516*, 231–233.
- (49) Falenty, A.; Kuhs, W. F. Self-Preservation” of CO₂ Gas Hydrates—Surface Microstructure and Ice Perfection. *J. Phys. Chem. B* **2009**, *113*, 15975–15988.
- (50) Monreal, I. A.; Devlin, J. P.; Maşlakçı, Z.; Çiçek, M. B.; Uras-Aytemiz, N. Controlling Nonclassical Content of Clathrate Hydrates Through the Choice of Molecular Guests and Temperature. *J. Phys. Chem. A* **2011**, *115*, 5822–5832.
- (51) Consani, K. Infrared Bands of Acetone in Solid Argon and the Structure II Clathrate 2-Acetylene/Acetone/17-Water. *J. Phys. Chem.* **1987**, *91*, 5586–5588.
- (52) Shin, S.; Kang, H.; Kim, J. S.; Kang, H. Phase Transitions of Amorphous Solid Acetone in Confined Geometry Investigated by Reflection Absorption Infrared Spectroscopy. *J. Phys. Chem. B* **2014**, *118*, 13349–13356.
- (53) Hagen, W.; Tielens, A. G. G. M.; Greenberg, J. M. The Infrared Spectra of Amorphous Solid Water and Ice I_c between 10 and 140 K. *Chem. Phys.* **1981**, *56*, 367–379.
- (54) Vishwakarma, G.; Malla, B. K.; Chowdhury, S.; Khandare, S. P.; Pradeep, T. Existence of Acetaldehyde Clathrate Hydrate and Its Dissociation Leading to Cubic Ice under Ultrahigh Vacuum and Cryogenic Conditions. *J. Phys. Chem. Lett.* **2023**, *14*, 5328–5334.
- (55) Lisgarten, N. D.; Blackman, M. The Cubic Form of Ice. *Nature* **1956**, *178*, 39–40.
- (56) Kouchi, A.; Kuroda, T. Amorphization of Cubic Ice by Ultraviolet Irradiation. *Nature* **1990**, *344*, 134–135.
- (57) Vishwakarma, G.; Malla, B. K.; Reddy, K. S. S. V. P.; Ghosh, J.; Chowdhury, S.; Yamijala, S. S. R. K. C.; Reddy, S. K.; Kumar, R.; Pradeep, T. Induced Migration of CO₂ from Hydrate Cages to Amorphous Solid Water under Ultrahigh Vacuum and Cryogenic Conditions. *J. Phys. Chem. Lett.* **2023**, *14*, 2823–2829.
- (58) Wooldridge, P. J.; Richardson, H. H.; Devlin, J. P. Mobile Bjerrum Defects: A Criterion for Ice-like Crystal Growth. *J. Chem. Phys.* **1987**, *87*, 4126–4131.
- (59) Moudrakovski, I. L.; Udachin, K. A.; Alavi, S.; Ratcliffe, C. I.; Ripmeester, J. A. Facilitating Guest Transport in Clathrate Hydrates by Tuning Guest-Host Interactions. *J. Chem. Phys.* **2015**, *142*, No. 074705.
- (60) Ohgaki, K.; Nakatsuji, K.; Takeya, K.; Tani, A.; Sugahara, T. Hydrogen Transfer from Guest Molecule to Radical in Adjacent Hydrate-Cages. *Phys. Chem. Chem. Phys.* **2008**, *10*, 80–82.
- (61) Sugahara, T.; Kobayashi, Y.; Tani, A.; Inoue, T.; Ohgaki, K. Intermolecular Hydrogen Transfer between Guest Species in Small and Large Cages of Methane + Propane Mixed Gas Hydrates. *J. Phys. Chem. A* **2012**, *116*, 2405–2408.
- (62) Goldberg, P. Free Radicals and Reactive Molecules in Clathrate Cavities. *Science* **1963**, *142*, 378–379.
- (63) Takeya, K.; Tani, A.; Yada, T.; Ikeya, M.; Ohgaki, K. Electron Spin Resonance Study on γ -Ray-Induced Methyl Radicals in Methane Hydrates. *Jpn. J. Appl. Phys.* **2004**, *43*, 353.
- (64) Bauer, R. P. C.; Ravichandran, A.; Tse, J. S.; Appathurai, N.; King, G.; Moreno, B.; Desgreniers, S.; Sammynaiken, R. In Situ X-Ray Diffraction Study on Hydrate Formation at Low Temperature in a High Vacuum. *J. Phys. Chem. C* **2021**, *125*, 26892–26900.